Comparison of different supervised neural network architectures in detecting motion corrupted Photoplethysmogram signal

Purbadri Ghosal*
EEE Department
Pondicherry Engineering College, Puducherry, India,
purbadrighosal@gmail.com

S. Himavathi
EEE Department
Pondicherry Engineering College, Puducherry, India,
himavathi@ptuniv.edu.in

E. Srinivasan
ECE Department
Pondicherry Engineering College, Puducherry, India,
esrinivasan@pec.edu

***Abstract*—Finger pulse signal, popularly known as Photoplethysmogram (PPG), can provide important information on circulatory functions in the human body. PPG signal is prone to motion artifact (MA) due to peripheral body movement. Hence pre-processing is an essential prerequisite before its accurate analysis. Pre-processing becomes difficult when only the corrupted PPG signal is available without any accelerometer reading. This paper aims to address this issue using intelligent techniques. Several supervised neural network (NN) architectures are designed and trained to identify clean and corrupted beats without needing a separate reference noise signal. A number of clinical features are derived from the beats. The unlabelled clinical feature data obtained is segregated into clean and noisy beats based on statistical analysis and is labeled accordingly for training and testing the NN architectures. The NNs are trained to identify clean and corrupted beats. The algorithms were validated with two standard open-source databases. The comparison of the networks is based on the accuracy of MA detection on the test dataset and the total computation time. The Convolution Neural Network performs well in terms of accuracy but requires higher computation time. The results obtained are promising and can aid the development and design of convenient wearable devices to monitor cardiovascular parameters in any environment.**

Keywords— Neural Networks; Biomedical signal processing; Peak detection; Motion artefact; Photoplethysmogram

I. INTRODUCTION

In recent times increasing health care awareness and rising healthcare costs have accelerated research in wearable vital parameter monitoring. Of different other vitalities, continuous heart rate monitoring is an important one that needs to be assessed in our day-to-day life. Huge literature can be found with ECG signals for determining the heart rate. But for ambulatory monitoring, acquiring ECG signal is challenging owing to the complexities involved with the electrodes. Hence PPG signal is used in these wearable devices e.g. Fitbit Charge [1], Samsung Simband, Apple Watch [3] etc. The popularity of the PPG sensor is mainly due to its low cost, non-invasiveness and measurement sites which are generally the peripheral parts of the body where signal collection becomes very easy while doing day to day activities. [2] emphasized that Security is an important issue in current and next-generation networks. Blockchain will be an appropriate technology for securely sharing information in next-generation networks. Digital images are the prime medium attacked by cyber attackers.

A PPG is a light sensor that measures the intensity of light reflected or transmitted through the skin caused by changes in arterial blood volume. Some critical factors on which the amplitude of the PPG signal depends are the amount of blood rushing into the peripheral vascular bed, skin pigmentation, ambient light, and the wavelength used to illuminate the blood [4]. However, with so many advantages comes a challenge of motion artefact contamination which disturbs the original morphology of the signal and leads to erroneous measurements of the vitalities [5]. Hence to increase the robustness of PPG-based vital parameter calculation, algorithms for removing motion artefact assumes importance.

Different techniques for motion artefact reduction in time domain is implemented using adaptive filtering methods. Some other techniques utilized the frequency domain of the signal viz., wavelet transformation techniques, IMAT [7], SpaMa [8], WFPV, and MC-SMD. Some other popular methods implemented for pre-processing PPG signals are Independent Component Analysis (ICA) [11], Window's adaptive noise cancellation (ANC) [12], cycle by cycle Fourier series analysis (CFSA) technique [13], Principal Component Analysis (PCA) [14], Empirical Mode Decomposition (EMD) [15], Wiener filtering [16] etc. However, most of these works require at least the availability of accelerometer data or consecutive ECG signal data. The major challenge of artefact removal occurs when the corrupted PPG signal alone is available. Also there is no labelled dataset available to train any intelligent techniques to distinguish between clean

and corrupted beats. This work attempts to address this complex problem with the use of artificial neural networks. The use of artificial intelligence in bio signal analysis is a topic of interest for many researchers. Various neural network architectures were used in recent times for cardiac signal processing. Deep Convolutional Networks was designed for atrial fibrillation detection from ECG signal [17], a multi-layer perceptron (MLP) network was optimized for mental stress assessment from PPG Signal [18], Support Vector Machines were used for classification of ECG Data with missing values [19], artificial neural networks were designed to detect anomalies present in ECG signals [20] etc. This paper proposes the use of intelligent networks to identify corrupted beats using standalone PPG data. No additional data viz., accelerometer data or ECG data is assumed to be known. Different statistical analysis were performed to differentiate between corrupted and normal beats for training the networks. Various learning neural networks with varied activation functions are designed for predicting a motion artefact corrupted beat. The performances of the networks designed are compared in terms of accuracy, mean square error and time period of execution.

The paper is organized as follows. Section 2 outlines the various steps involved in pre-processing, identification of clean and corrupted beats, feature extraction, creation of the datasets needed for training and testing. Section 3 details the databases used, digital filtering done on the raw data, computation of statistical parameters for labelling each beat as clean or corrupted and extraction of features needed for training. Section 4 presents the various neural architectures designed and compares the performance of the networks in terms of accuracy and computational speed. Section 5 draws the major conclusions and contributions of the work carried out.

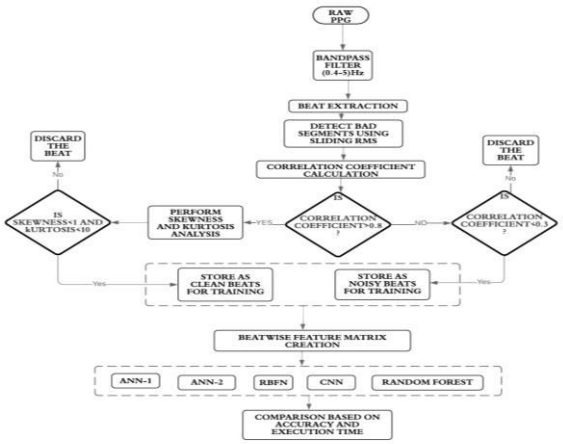

Figure. 1 Work flow diagram

II. METHODOLOGY

The steps adopted to obtain a data set segregating clean and corrupted beats of the input PPG signal is discussed in this section. The raw PPG signal is extracted from two standard databases which contain motion artefact contaminated data. A bandpass digital filter is designed to eliminate frequency components outside the area of interest. The output of the bandpass filter is used to identify the peak and foot of the beats. The extracted beats are normalized and using correlation coefficient classified as clean or corrupted beats. Finally, various neural network architectures are designed using the same training and testing data sets. The networks were compared based on accuracy and the total execution time for the network. The workflow diagram is given in Figure.1.

A. Data Collection

Two publicly available datasets are being used in this work. One is the IEEE Signal Processing Cup 2015 [21]. This dataset is divided into two parts: a training dataset and a test dataset. The other data set is the published 'Heart rate estimation during physical exercises' [22] dataset herein referred to as the PPG_Motion dataset.

The IEEE training and testing dataset were recorded with a wrist-worn device, which included a PPG sensor (two-channel) with LED having a wavelength of 515 nm and a three-axis accelerometer. It also has the record of ECG signal obtained simultaneously, providing the heart rate ground truth. The data from 12 different people with 18-35 age group were recorded while running on a treadmill at varying speeds with a sampling rate of 125 Hz. The IEEE_Test dataset contains the record of 8 different subjects of age group 19–58 years, followed the same hardware setup. However, the data collection protocol for the IEEE_Test dataset consists of 10 sessions. In the first 4 sessions, various arm exercises and the last 6 sessions, intensive arm movements were performed by the subjects.

PPG_Motion dataset was also recorded with a wrist-worn device, including PPG and an ECG sensor. It contains data recorded from 8 subjects aged 22–32 years. They were made to perform outdoor physical activities such as walking, running, biking by simulating the same speed of those activities on the treadmill and exercise bike.

B. Digital Filtering

A 2nd order bandpass filter with a passband frequency of 0.4Hz to 5Hz is designed as the first stage of pre-processing the raw signal. The frequency band remains the main band of interest for heart rate. Not much of a difference is being noticed pre and post-filtering as the motion artefact is not only in the

filtered frequency range. The frequency of the PPG signal is s 0.5 to 5 Hz, while for motion artefacts it is 0.01 to10 Hz [23]. Fig. 2 shows the frequency response of the filter. Fig.3 shows the PPG signal before and after filtering.

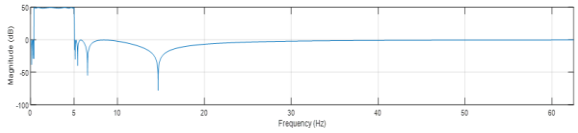

Figure. 2 Frequency response of the filter

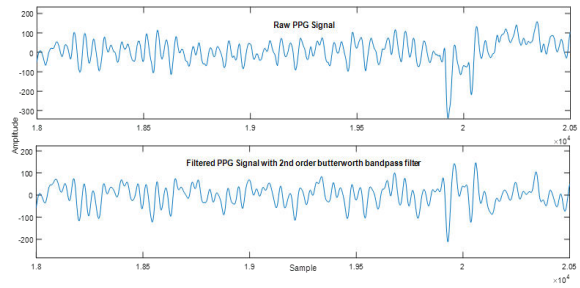

Figure. 3 PPG signal before and after digital

C. Peak Foot Detection Algorithm

In the current work, the quality of every individual beat is examined to identify the presence of motion artefacts if any. Hence for separating each beat from a continuous signal, the systolic peaks and foot are detected first. [9] discussed about detection of leukaemia using a small picture handling method that distinguishes between red blood cells and young white cells. Visual examination of minuscule photos by looking at alterations such as surface, calculation, shading, and measurable research of photographs is now the only recognisable proof of blood trouble..

D. Beatwise segmentation

For beatwise feature calculation, a n x m dimension matrix was constructed with each PPG beat, where n is the number of PPG beats in the signal and m is the length of the beats after necessary zero padding. All the beats are aligned to a common point of reference, the systolic peak where the signal-to-noise ratio (SNR) is maximum. The part of signal between two foots is considered as a beat. After extraction, the kth beat vector may be represented as:

$B_k = [b_{k1}\, b_{k2} \ldots . b_{km}]^T$ (1)

Where, b_{kj} represents j^{th} sample of k^{th} beat of length m. Zero padding was done at both ends of the systolic peak, wherever necessary, to make the length of the beats equal. The final beat matrix B can be represented as:

$$B = \begin{bmatrix} b_{11}\ b_{21} \cdots & b_{n1} \\ b_{12}\ b_{22} \cdots & b_{n2} \\ . & \\ . & \\ b_{1m} \ \ldots\ldots & b_{nm} \end{bmatrix} \quad (2)$$

E. Clean and Corrupted Beat File Creation Using Statistical Parameters

Statistical parameters quantitatively summarize a large dataset and help us create a scope for efficient categorization within the dataset. Such parameters used in previous literatures and the current work are listed below:

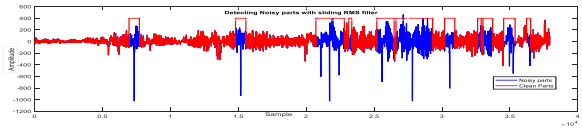

a) Detecting Bad segment using sliding RMS window:

RMS is the root-mean-square value of a signal. If the signal amplitudes vary greatly due to noises present, the RMS value is also going to vary along with it. [10] discussed that Liver tumor division in restorative pictures has been generally considered as of late, of which the Level set models show an uncommon potential with the advantage of overall optima and functional effectiveness. RMS is calculated from each window by the following formulae:

$$\sqrt{\frac{1}{N}\sum_{n=0}^{N-1}|x[n]|^2} \quad (3)$$

Where, N is the length of each window, x (n) are the amplitudes of the samples present inside the window. Fig. 4 shows the portion detected as noisy samples and the portion detected as clean samples after sliding window based RMS analysis. The signal is then given for extraction and storing beat matrix B (from section 3.3). However the noisy beats are marked noisy and the clean beats are marked clean in a separate target vector file based on the RMS analysis at this stage.

b) Correlation Coefficient:

The correlation coefficient value of consecutive beats can give an idea about the extent of corruptness in the beats. In a resting PPG signal without motion artefact, there is not much variation between consecutive beats, which makes the beats morphologically look nearly identical with each other. Hence the COF array formed with no motion artefact present will have values close to 1.

The more a signal is contaminated with motion artefact, the less will be the correlation between consecutive beats. Correlation coefficients>0.8 are used to select clean beats for training. Further skewness and kurtosis are also calculated following the protocol described in [26]. Correlation coefficient <0.3 signifies consecutive beats are highly different from each other. Those beats were used for training as noisy beats.

The COF between each column of the B matrix, which represents the consecutive beats of the dataset, is calculated by the formula:

$$COF(a,b) = \frac{1}{M-1}\sum_{i=1}^{M}\left(\frac{a-\mu_a}{\sigma_a}\right)\left(\frac{b-\mu_b}{\sigma_b}\right) \quad (4)$$

Where, M is the total number of samples in two consecutive beats here represented as a and b, μ_a and μ_b are the respective means of the beats and σ_a and σ_b are the respective standard deviation of the beats. The consecutive beats COF are stored in an array of dimension 1xN, where N is the number of beats-1. This

array is further utilized in updating the target vector file for training the network.

b) Skewness and Kurtosis:

This parameter give information on the shape of the data distribution around a central tendency. From the matrix B the skewness, and kurtosis are calculated using Eqs. 5 and 6, respectively,

$$\text{skewness} = \frac{\frac{1}{n}\sum_{i=1}^{n}(x_i-\bar{x})^3}{std^3} \quad (5)$$

$$\text{kurtosis} = \frac{\frac{1}{n}\sum_{i=1}^{n}(x_i-\bar{x})^4}{std^4} \quad (6)$$

Where $\bar{x}$ is the mean value of each column of matrix B. Without the presence of motion artefact, the kurtosis, skewness for each cycle is almost equal [27]. These values are then calculated and set as thresholds for the comparison algorithm. If there is movement, the amplitude of the PPG signal changes greatly, and consequently, the statistical parameters vary, and the beat is marked as corrupt.

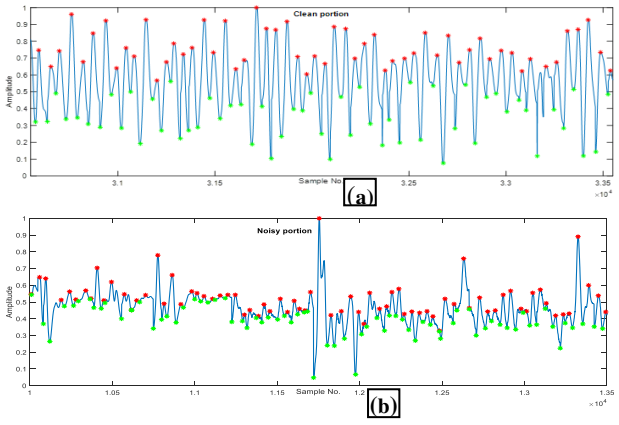

Figure. 5 Training dataset a) clean portion and b) noisy portion

Fig. 5a shows Fig 5b shows the portion of PPG data labelled as the clean part in the target vector and the portion of PPG data affected with motion artefact labelled as the noisy part in the target vector separated after the statistical analysis.

F. Feature Calculation:

Based on the fiducial points as shown in Fig. 6, useful clinical features were extracted to form a beat wise feature set matrix which would be the input to the neural network. The relationship between PPG features and clinical cardiovascular parameters were earlier studied in [28]. The features extracted are:

Feature 1: Systolic Amplitude (A): It is the amplitude of the systolic peak which is used for finding the stroke volume and also gives an idea about the health of blood vessels;

Feature 2: Pulse Width (C): It is the width of the beat measured at half systolic amplitude. Pulse Width is used for determining systemic vascular resistance.

Feature 3: Systolic Peak to Systolic Peak distance (B): It is the distance between two consecutive systolic peaks. It correlates closely with the R-R interval of ECG, which can be used for finding heart rate.

Feature 4: Pulse Interval (D): It is the distance between the two feet of a beat. The ratio of PI with systolic amplitude gives a clear idea of a person's cardiovascular system.

Feature 5: Pulse Area: It is the area under the PPG curve.

Feature 6: Half systolic peak height: It is half the length of Systolic Amplitude. The ratio of the diastolic peak height to the systolic peak height (E) can be used to calculate the arterial stiffness.

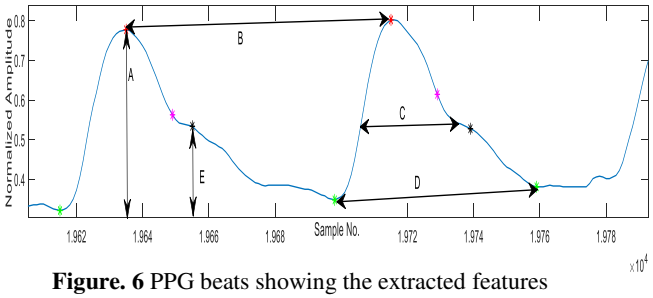

Figure. 6 PPG beats showing the extracted features

G. Feature Analysis and Transformation

The features calculated were extensively studied and the following transformation were performed to optimize the data:

i) Outliers: The box plot in Fig. 7 shows the presence of outliers in the training dataset [29].

ii) Scale: Gradient descent algorithms require data to be scaled. According to the formula for gradient descent below:

$$\theta_j := \theta_j - \alpha\frac{1}{m}\sum_{i=1}^{m}(h_\theta(x^{(i)}) - y^{(i)})x_j^{(i)} \quad (7)$$

Where X is the input feature value which is proportional to the step size of the gradient descent. Hence, the difference in ranges of features will cause different step sizes for each feature. To ensure that the minima can be found swiftly, the step updates are kept at the same rate for all the features. Two kinds of scaling are done here:

(a) *Data Normalization*: It is the rescaling of the data from the original range so that all values are within the new range of 0 and 1. A value is normalized as follows:

$$Normalized\ value = \frac{Actual\ value - Minimum\ Value}{Maximum\ value - Minimum\ value} \quad (8)$$

(b) *Data Standardization*: The data are rescaled so that the mean of observed values is 0 and the standard deviation is 1. Standardization is done by the following formula:

$$Standardized\ value = \frac{Actual\ value - Mean}{Standard\ deviation} \quad (9)$$

Where the mean is calculated as:

$$Mean = \frac{\sum_i^N x_i}{N} \quad (10)$$

And the standard deviation is calculated as:

$$Standard\ deviation = \sqrt{\frac{\sum_i^N (x_i - Mean)^2}{N}} \quad (11)$$

Where x is the sample value at i^{th} instance and N is the total number of samples.

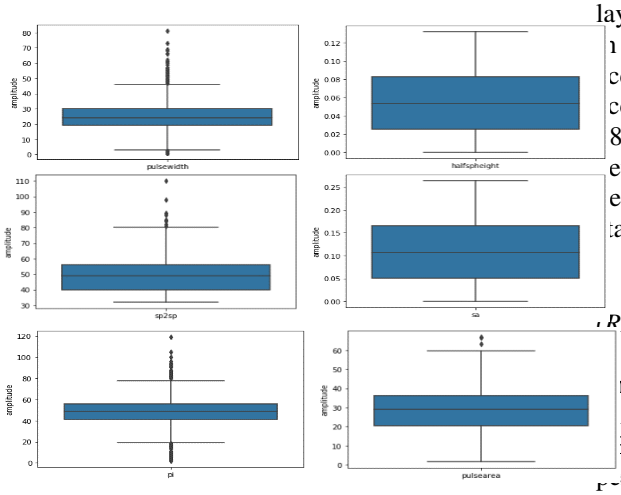

Figure. 7 Boxplot of PPG features showing the presence of outliers

H. Supervised Networks

1) Network 1: Feedforward Backpropagation Network I (ANN-1)

The scaled feature matrix described in the earlier section is used as the input to the 3-layer Feed forward backpropagation network [30] with an architecture of 6-6-1. The input layer uses the sigmoid activation function followed by another sigmoid activation function for the second hidden layer, and the output layer uses rectified linear activation function (ReLU). Input feature matrix had a dimension of 3850 x 6, where 3850 is the total number of beats and 6 is the total number of features used. For training, 80% of the dataset, i.e., 3080 beats were used. For testing, 770 (20%) beats were used. The network is trained for a total of 100 epochs. The training accuracy is found to be 57.20 %, and the testing accuracy is 56.49 %. The MSE for the test set was 6.6015. Further epoch didn't change the MSE, and this is the minimum MSE we achieved for this architecture.

This high MSE and low accuracy are solved by giving ReLU that can be given in the hidden layers [31]. The next network thus interchanges the activation functions to study the effect of the activation function. [6] discussed about diabetic retinopathy from retinal pictures utilizing cooperation and information on state of the art sign dealing with and picture preparing. The Pre-Processing stage remedies the lopsided lighting in fundus pictures and furthermore kills the fight in the picture.

2) Network 2: Feedforward Backpropagation Network Ii (ANN-2)

The architecture of this network remains the same as the previous network. The only difference is here ReLU activation function was given in the hidden layers and the sigmoid activation function was given n the output layer. A significant improvement in ccuracy was seen for this network. Training ccuracy was 88.83% and testing accuracy was 8.75% with a testing MSE of 0.2914. This trained etwork can be deployed to real world normalized eats to classify them as noisy or clean beats in a tandalone device.

3) Network 3: Radial Basis Function Network (RBFN)

n this network, the input signal is transformed into other form, to get linear separability of the data. BFN is structurally the same as a multi-layer erceptron network i.e., it is composed of input, hidden, and output layers [32]. However, in this network, the number of hidden networks is limited to one. The number of neurons present in the hidden node is dependent upon the value spread that we give as an input to the function. The larger spread means the function approximation is smoother. Also, too small a spread means might not generalize well [33]. The cross-validation technique is applied to find the optimum value of the spread. It is observed the spread value of 0.8 needed a total of 344 hidden layer neurons and gave the minimum mse. A non-linear transfer function is applied to this hidden layer. The training accuracy for this network

was 83.59% and the testing accuracy for this network was 82.44%.

4) Network 4: Convolution Neural Network (CNN)

Convolution neural network [34] performs best among all the deep learning networks. Convolution neural network works on image processing. Hence each beat is saved as an image in two groups viz. clean and noisy for training the network. The figures have a resolution of 432 x 288 pixels with 72 dpi (72 pixels per inch figures). The main advantage of this network is that it is independent of any signal processing algorithms and decides the extent of corruption of the beats simply by looking into its morphology. The training accuracy was 91.12 % and the testing accuracy was 90.30%.

5) Network 5: Random Forest Classifier

Random forest is a supervised learning algorithm. It is a collection of decision trees, usually trained with the "bagging" method [35]. In the bagging method, a combination of learning models increases the overall result. In this network, the best feature among a random subset of features is searched while splitting a node. Therefore, in a random forest, only a random subset of the features is taken into consideration by the algorithm for splitting a node. Training accuracy was 85.55% and testing accuracy was 84.37% for this network.

The following table shows the comparison of the networks based on the accuracy of beat wise motion artefact detection on the test dataset and the total execution time.

Table 1: Comparing the performances of the networks in terms of accuracy and execution time

Network name	Test Accuracy	Execution time (sec)
ANN-1(Network 1)	57.20%	34.2343
ANN-2 (Network 2)	89.83%	32.1718
RBFN (Network 3)	81.44%	35.63
CNN (Network 4)	92.30%	204.2812
Random Forest Classifier (Network 5)	84.37%	1.314978

Table 1 shows that the CNN network performs best in terms of accuracy however it takes the most amount of time among all other networks. Random forest algorithm is the fastest among all with medium accuracy.

III. Results and Discussions

The main challenge of this work is to identify the presence of motion artefact corrupted beats in a standalone PPG signal (without the presence of accelerometer signal or ECG signal). Here supervised networks are trained using beats which are labelled by various statistical parameters. Although the supervised neural network performed quite well (average accuracy>80% except for Network 1), it somehow misses a few critical beats. Exploratory data analysis shows not much difference in statistical measure was there between the features of the training set and the test set. Detailed statistical evaluations of the two groups are shown in Table 2. The mean, minimum and maximum values of different features for clean and noisy datasets are tabulated side by side for comparison. The features do not show striking differences from each other. The input to networks 1-3 and 5 are only these features. So the supervised network might have failed to understand the differences based on these time-domain features.Hence if the accelerometer signal were utilized, the training data with clean beats and noisy beats with clean beats and noisy beats would have been more accurately grouped. The future scope of this work can be delving deep into the accelerometer signal.

IV. CONCLUSION

This paper proposes the use of supervised networks to identify corrupted beats using standalone PPG data. No accelerometer data or ECG data are used in this work. A
variety of statistical parameters are carefully examined to quantify the nature of the beats i.e., the extent of its motion artefact corruption. The main aim of this work is to examine how various supervised neural networks perform in assessing beat quality. Five supervised neural networks with varied activation functions are designed for predicting a motion artefact corrupted beat. The performances of the networks designed are compared in terms of accuracy and time period of execution. CNN performed the best among all other networks in terms of accuracy (90.3%) however it
took a lot of time for execution. Thus for a problem like this, and real-time quality assessment, it can be concluded that Random Forest Classifier with necessary feature engineering will provide the most optimised solution (Accuracy 83.52%).Another challenge faced is related to the available databases. The length of each session's recording can be considered short (less than 120 min each). Hence, to address a wider range of challenging signal artefacts, signal with variety of movements would possibly do better.

REFERENCES

[1] Muoio D., 'Fitbit launches large-scale consumer health study to detect a-fib via heart rate sensors, algorithm', mobi health news, 06 May. 2020.
URL: https://www.mobihealthnews.com/news/fitbit-launches-large-scale-consumer-health-study-detect-fib-heart-rate-sensors-algorithm

[2] Christo Ananth, Denslin Brabin, Sriramulu Bojjagani, "Blockchain based security framework for sharing digital images using reversible data hiding and encryption", Multimedia Tools and Applications, Springer US, Volume 81,Issue 6, March 2022,pp. 1-18

[3] Isakadze N, Martin S.S., "How useful is the smartwatch ECG?",Trends in Cardiovascular Medicine,30(7) 2020: 442-448,ISSN 1050-1738, https://doi.org/10.1016/j.tcm.2019.10.010.

[4] Reisner A, Shaltis PA, McCombie D, Asada HH, "Utility of the photoplethysmogram in circulatory monitoring", Anesthesiology 108(5), 2008: 950-958. DOI: 10.1097/ALN.0b013e31816c89e1

[5] Paliakaitė, B., Petrėnas, A., Sološenko, A., & Marozas, V, "Modeling of artifacts in the wrist photoplethysmogram: Application to the detection of life-threatening arrhythmias". Biomedical Signal Processing and Control, 66, 2021. DOI: https://doi.org/10.1016/j.bspc.2021.102421

[6] Christo Ananth, D.R. Denslin Brabin, Jenifer Darling Rosita, "A Deep Learning Approach To Evaluation Of Augmented Evidence Of Diabetic Retinopathy", Turkish Journal of Physiotherapy and Rehabilitation, Volume 32,Issue 3, December 2021,pp. 11813-11817.

[7] Mahdi B. et. al., "Heart Rate Tracking using Wrist-Type Photoplethysmographic (PPG) Signals during Physical Exercise with Simultaneous Accelerometry",
IEEE Signal Processing Letters 23(2) ,2015. DOI: 10.1109/LSP.2015.2509868

[8] Salehizadeh SM, Dao D, Bolkhovsky J, Cho C, Mendelson Y, Chon KH. , "A Novel Time-Varying Spectral Filtering Algorithm for Reconstruction of Motion Artifact Corrupted Heart Rate Signals During Intense Physical Activities Using a Wearable Photoplethysmogram Sensor." Sensors (Basel). 16(1):10, 2015. DOI: 10.3390/s16010010. PMID: 26703618; PMCID: PMC4732043.

[9] Christo Ananth, P. Thenmozhi, Stalin Jacob, Dr.A. Anitha, "Leukemia Blood Cancer Detection Using MATLAB", Turkish Journal of Physiotherapy and Rehabilitation, Volume 32,Issue 3, December 2021,pp. 10257-10261.

[10] Christo Ananth, M Kameswari, Densy John Vadakkan, Dr. Niha.K., "Enhancing Segmentation Approaches from Fuzzy-MPSO Based Liver Tumor Segmentation to Gaussian Mixture Model and Expected Maximization", Journal Of Algebraic Statistics, Volume 13, Issue 2, June 2022,pp. 788-797.

[11] Kim B.S., Yoo S.K., "Motion artifact reduction in photoplethysmography using independent component analysis." IEEE Trans. on Biomed. Eng., 53(3), 2006: 566 – 568.

[12] Kim S. H., Ryoo D. W. and Bae C., "Adaptive Noise Cancellation Using Accelerometers for the PPG Signal from Forehead," 29th Annual International Conference of the IEEE Engineering in Medicine and Biology Society, 2007, pp. 2564-2567, DOI: 10.1109/IEMBS.2007.4352852.

[13] Reddy K.A., George B., Kumar V.J., "Use of fourier series analysis for motion artifact reduction and data compression of photoplethysmographic signals." IEEE Trans. on Inst. Meas., 58(5), 2009: 1706 - 1711.

[14] Ram M.R., Madhav K.V., Krishna E.H., Reddy E.H., and Reddy K.A., "Use of Multi-Scale Principal Component Analysis for Motion Artifact Reduction of PPG Signals", IEEE Recent Advances in Intelligent Computational Systems (RAICS), India, 22-24 Sept. 2011, pp. 425430.

[15] Sun X., Yang P., Li Y., Gao Z. and Zhang Y., "Robust heart beat detection from photo plethysmography interlaced with motion artifacts based on Empirical Mode Decomposition." IEEE-EMBS Inter. Conf. on Biomed. and Health Informat. (BHI 2012), Hong Kong and Shenzhen, China, pp. 775-778, 2-7 Jan 2012.

[16] Chung H, Lee H, Lee J. Finite State Machine Framework for Instantaneous Heart Rate Validation Using Wearable Photoplethysmography During Intensive Exercise. IEEE J Biomed Health Inform. Jul; 23(4), 2019:1595-1606. DOI: 10.1109/JBHI.2018.2871177

[17] Zhao, Z., Särkkä, S. & Rad, A.B. Kalman-based Spectro-Temporal ECG Analysis using Deep Convolutional Networks for Atrial Fibrillation Detection. J Sign Process Syst 92, 2020: 621–636. DOI: https://doi.org/10.1007/s11265-020-01531-4 year

[18] Prerita K., Sharma V.,"Mental Stress Assessment Using PPG Signal a Deep Neural Network Approach", IETE Journal of Research, 2020, DOI: 10.1080/03772063.2020.1844068

[19] Maryamsadat H., Al-Haddad S. A. R., Prasad Singh Y., Shaiful J. H. & Ahmad F.A.A,"Multiclass Support Vector Machines for Classification of ECG Data with Missing Values", Applied Artificial Intelligence, 29(7), 2015: 660-674, DOI: 10.1080/08839514.2015.1051887

[20] Tomasz A., "Machine Learning Techniques Applied to Data Analysis and Anomaly Detection in ECG Signals", Applied Artificial Intelligence, 30(6), 2016: 610-634, DOI: 10.1080/08839514.2016.1193720

[21] Zhilin Z., Zhouyue Pi, Benyuan L., ''TROIKA: A General Framework for Heart Rate Monitoring Using Wrist-Type Photoplethysmographic Signals During Intensive Physical Exercise,'' IEEE Trans. on Biomedical Engineering, 62(2),2015 pp. 522-531

[22] Jarchi D. and Casson A. J., "Description of a database containing wrist PPG signals recorded during physical exercise with both accelerometer and gyroscope measures of motion," Data, 2(1),2016: 1.
[23] Rojano, J.F.; Isaza, C.V., "Singular value decomposition of the time-frequency distribution of PPG signals for motion artifact reduction". Int. J. Signal Process. Syst. 2016, 4, 475–482
[24] Deborah R., Jonathan K, Ehrman, G.L., Meir M. Chapter 6 "General Principles of Exercise Prescription.", ACSM's Guidelines for Exercise Testing and Prescription. 6, 2018: 143-179.
[25] "Bradycardia: Slow heart rate". American Heart Association. http://www.heart.org/HEARTORG/Conditions/Arrhythmia/AboutArrhythmia/Bradycardia-Slow-Heart-Rate_UCM_302016_Article.jsp. Accessed Dec. 28, 2016.
[26] Hanyu S, Xiaohui C "Motion artifact detection and reduction in PPG signals based on statistics analysis. 29th Chinese control and decision conference (CCDC), pp 3114–3119, 2017
[27] Pollreisz, D., TaheriNejad, N. Detection and Removal of Motion Artifacts in PPG Signals. Mobile Netw Appl (2019). https://doi.org/10.1007/s11036-019-01323-6
[28] Elgendi M. On the analysis of fingertip photoplethysmogram signals. Curr Cardiol Rev.; 8 (1), 2012:14-25. DOI: 10.2174/157340312801215782, 2012
[29] Georgy L. Shevlyakov,H. O. ,"Applications to Exploratory Data Analysis: Detection of Outliers". Wiley Series in Probability and Statistics, 2016, 231–254. doi:10.1002/9781119264507.ch9
[30] Moller M.F., "A scaled conjugate gradient algorithm for fast supervised learning", Neural Networks, 6(4), 1993: 525-533.
[31] Glorot, X., Bordes, A. & Bengio, Y., "Deep Sparse Rectifier Neural Networks." Proceedings of the Fourteenth International Conference on Artificial Intelligence and Statistics, in Proceedings of Machine Learning Research 15, 2011:315-323 Available from http://proceedings.mlr.press/v15/glorot11a.html.
[32] Amir S. A., Chapter 7 – "Numerical Modeling and Simulation", Numerical Models for Submerged Breakwaters, 2016: 109-126, ISBN 9780128024133, https://doi.org/10.1016/B978-0-12-802413-3.00007-9.
[33] Martin S, Choi CT. "On the influence of spread constant in radial basis networks for electrical impedance tomography". Physiol Meas. 37(6), 2016:801-19. doi: 10.1088/0967-3334/37/6/801.
[34] S.C.B. Lo et. al., 'Artificial convolution neural network for medical image pattern recognition',Neural Networks, 8(7),8,1995:1201-1214,ISSN 0893-6080
[35] Paul A., Mukherjee D. P., Das P., Gangopadhyay A., Chintha A. R. and Kundu S., "Improved Random Forest for Classification," IEEE Transactions on Image Processing, 27(8),2018: 4012-4024, doi: 10.1109/TIP.2018.2834830.